



Double-sided wet fabric evaporator utilizing wind and solar energy efficiently—Simulation modeling and feasibility of evaporator

T. Nosoko*, S. Gima, H. Minakuchi, K. Ameku, K. Irabu

*Department of Mechanical Systems Engineering, University of the Ryukyus, Senbaru 1, Nishihara, Okinawa 903-0213, Japan
Tel. +81 (98) 895-8616; Fax +81 (98) 895-8636; email: yongrang@tec.u-ryukyu.ac.jp*

Received 10 September 2009; Accepted 22 December 2009

ABSTRACT

A double-sided wet fabric evaporator is suggested, which has a potential to concentrate seawater up to a high concentration in a very short fabric length of around 2 m. Model simulations show that evaporation from both sides of the fabric effectively cools the fabric which gains a large amount of heat from the surroundings for the nighttime and emits a small amount of heat loss to surroundings for the sunny daytime. Under the subtropical and maritime climate conditions of Okinawa Island, the evaporator produces evaporation amount of 5.23 kg/day-m² fabric on average. The solar-aided evaporation accounts for 63% of the total evaporation amount of 6.01 kg/day-m² fabric in humid and sunny July, and it does for 24% of the total amount of 5.03 kg/day-m² fabric in less-humid and cloudy January.

Keywords: Evaporation; Concentration; Seawater; Solar energy; Wind

1. Introduction

Cooking salt rich in minerals which were originally dissolved in seawater is preferred by health-minded consumers in Japan and other countries. The salt production however requires the evaporation of large volumes of water from seawater. Large amounts of heavy oil and firewood are often used as fuel to heat up and evaporate seawater, and this greatly boosts up the amount of CO₂ emission and the salt production cost.

In many saltworks in Japan, seawater is concentrated by evaporation to produce brine, and then the brine is further evaporated to deposit NaCl, Mg and other minerals, while gypsum is removed from the brine (ref. SSWSJ & SSRF [1]). In this first process of evaporation, it is desirable to concentrate seawater to 14 wt% over which gypsum begins to deposit. The concentration to 14 wt% requires the evaporation of 78% of

water contained in seawater of 3.4 wt%, and therefore reductions of CO₂ emission and of the fuel are important in the first process.

To reduce the CO₂ emission and the production cost, multiple-effect, wind-aided and solar-aided evaporation processes have been applied to produce the brine (SSWSJ & SSRF [1], Sugi and Nakayama [2] and Nosoko *et al.* [3]). A wind-aided process used to be widely employed in salt production in Japan (SSWSJ & SSRF [1], and Sugi and Nakayama [2]). In that respect, multiple upside-down bamboos were tied to poles and cross bars, and seawater was fed to wet them throughout. The wind blowing through the rows of bamboos evaporates seawater as it flows down the surfaces of bamboos (Sugi and Nakayama [2]). Recently, Gilrom *et al.* [4] employed a net instead of bamboos for the wetted surface in order to reduce the volume of waste brine from inland desalination plants. The net was stretched in a zigzag pattern between upper and lower rows of horizontal bars to maximize its wetted surface area exposed to wind.

*Corresponding author.

Evaporation ponds or basins utilize solar energy in addition to wind, and are often employed in arid regions (Pancharatnam [5] and Manganaro and Schwartz [6]). Studies showed that shallow basins with smaller amounts of seawater achieve larger evaporation. Solar energy raises the temperature of smaller amount of seawater in a basin more rapidly to a higher level to widen the water-vapor pressure difference between the seawater and the ambient air, i.e. the driving force of evaporation, resulting in a larger amount of evaporation.

To make the layers of seawater extreme thin, open film-type evaporation process used to be widely applied to the salt production in Japan (SSWSJ & SSRF [1], and Sugi and Nakayama [2]). Gently sloping land surfaces of 0.38–0.57° from the horizontal were covered with clay layers to avoid seepage. Water was evaporated from seawater films as they flow down the sloping surfaces. The flow rates were set to be large enough to avoid dry patches appearing on the sloping surfaces. With such flow rates, the films require the entrance length of about 5 m or longer where seawater absorbs the solar energy and raises its temperature (or enthalpy). After its temperature begins to level off, the major evaporation occurs. With those flow rates the sloping surfaces of 20–40 m in length are needed to concentrate the flowing seawater to required concentrations (about 14 wt%).

Recently, several research groups studied the film-type evaporators with much shorter surfaces (Newell et al. [7], Kim et al. [8], Srithar and Mani [9] and Kim and Jenkins [10]). They circulated seawater between an evaporation surface and a storage tank to increase its concentration. These evaporators require an initial period to increase the temperature of circulating seawater before major evaporation occurs. Pumps circulating seawater consume larger amounts of electricity in these film-type evaporators of short lengths than longer evaporators.

In this paper, we suggest the double-sided wet fabric evaporator that has potential to utilize wind and solar energy more efficiently than the liquid-film-type ones, and explore its feasibility by means of model simulation. We present its evaporation rates predicted by applying the model to the maritime climate conditions of Okinawa Island at 26° latitude to the southeast of Chinese Continent.

2. Description of double-sided wet fabric evaporator

Fig. 1 shows a schematic of the double-sided wet fabric evaporator that we suggest in this paper. A rectangular fabric is stretched between horizontal bars and is tilted so that it collects solar radiation efficiently on the upper surface. Seawater is fed to the fabric at its top edge attached securely to the bar. The seawater soaks the

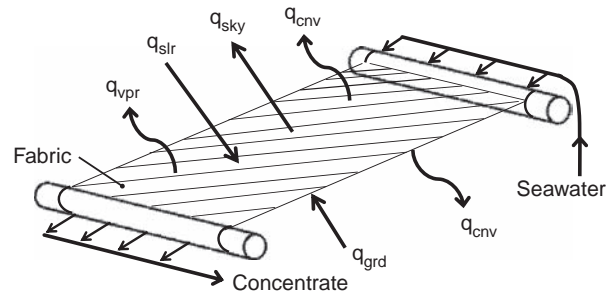


Fig. 1. Schematic of double-sided wet fabric evaporator and heat fluxes to/from evaporating fabric.

fabric throughout, and wind enhances evaporation from both the upper and lower surfaces as seawater flows in the fabric to the bottom edge where the concentrated seawater is collected and then conveyed to a reservoir. A hydrophilic material is employed for the fabric, so as to avoid dry patches appearing on the fabric at small feeding rates of seawater. With the small flow rates, seawater increases its concentration to required values as it evaporates in the fabric of 2 m length or less.

The short length of the fabric represents a major advantage of the suggested evaporator. The evaporators fixed to flexibly designed stands can be installed on difficult terrains. In comparison, the film-type evaporators require large land, moreover demanding an adequate gentle slope.

As shown later, the suggested evaporator shows a high performance even for the nighttime and daytime of low insolation, and thus it can be used not only in sunny seasons but also in cloudy seasons. This is another major advantage of the suggested evaporator.

3. Simulation model

The simulation model is based on the lumped capacitance method assuming for the evaporating fabric a heat exchange due to enthalpy carried in by the feeding seawater (q_{swt}), the insolation (q_{slr}), the convection from the surrounding air (q_{cnv}), the radiation from the ground (q_{grd}), the sky radiation (q_{sky}), and the loss of the latent heat of evaporation (q_{vpr}) at the fabric surface. The Biot number is calculated to be 0.08 or less from the used values of the heat transfer coefficient, thermal conductivity and thickness of seawater-soaked fabric, and this gives some validity of the employment of the lumped capacitance method. The different heat exchanges are

$$q_{swt} = m \cdot c \cdot (T_a - T) \quad (1)$$

$$q_{slr} = \alpha \cdot I \quad (2)$$

$$q_{cnv} = 2 \cdot h \cdot (T_a - T) \quad (3)$$

$$q_{\text{grd}} = \varepsilon \cdot \sigma \cdot (T_{\text{grd}}^4 - T^4) \quad (4)$$

$$q_{\text{sky}} = \varepsilon \cdot \sigma \cdot (T^4 - T_{\text{sky}}^4) \quad (5)$$

$$q_{\text{vpr}} = L \cdot m_e \quad (6)$$

$$m_e = 2 \cdot k \cdot (p - p_a) \quad (7)$$

The feed has a mass flow “ m ” while the rate of evaporation is “ m_e ”. The convection and the evaporation occur on both the upper and lower surfaces of fabric, and therefore the terms for them are doubled in Eqs. (3) and (7). Due to the lumped capacitance assumption, these heat exchanges are independent on the area of fabric.

An energy balance for the fabric of 1 m² area on each side then can be written as

$$M \cdot c \cdot (dT/dt) = q_{\text{swt}} + q_{\text{slr}} + q_{\text{cnv}} + q_{\text{grd}} - q_{\text{sky}} - q_{\text{vpr}} \quad (8)$$

The concentration of evaporating seawater S is the mean value of the concentration S_{in} of the influent seawater and the concentration S_{out} of the effluent. The concentration of the effluent is derived from mass balance for salt in evaporating seawater and can be expressed as

$$S_{\text{out}} = S_{\text{in}} \cdot \frac{m}{m - m_e} \quad (9)$$

The vapor pressure of seawater has been derived from the correlation fitting water saturation data given in JSME Databook [11] and from Witting [12]. They can be expressed as

$$p_w = \exp(23.5526 - 4030.18 / (T - 38)) \quad (10)$$

$$p/p_w = 1 - 0.5368S \quad (11)$$

The heat transfer coefficient h and the mass transfer coefficient k are based on correlations from Pancharatnam [5] and can be expressed as

$$h = 5.68 + 3.8 \cdot u \quad (\text{W/m}^2 \cdot \text{K}) \quad (12)$$

$$k = (19.3 + 10.8u) \cdot 10^{-9} \quad (\text{kg/m}^2 \cdot \text{s} \cdot \text{Pa} \text{ or } \text{s/m}) \quad (13)$$

The ground temperature is assumed to be equal to the air temperature T_a , and the sky temperature T_{sky} is based on a correlation from Berger et al. [13], which can be expressed as

$$(T_{\text{sky}}/T_a)^4 = 0.752 + 0.0048 \cdot (T_a - 273.15) \quad (14)$$

The solar radiation incident on the tilted fabric is assumed to be equal to the insolation on the horizontal I . The infrared emittance ε and the solar absorptance of the wetted fabric α are assumed to be 0.9 and 0.85,

respectively. The specific heat of the seawater-soaked fabric is assumed to be that of fresh water. A simple forward difference method has been used to calculate the fabric temperature $T(t)$ as time is incremented. When meteorological conditions are assumed to be constant, Newton’s method has been used to solve Eq. (8) in which the transient term on the left side is set to be zero.

An energy balance has been constructed for a single-sided evaporating fabric that exposes the upper surface to wind and thermally insulates the lower surface. It can be expressed as

$$M \cdot c \cdot (dT/dt) = q_{\text{swt}} + q_{\text{slr}} + \frac{1}{2} \cdot q_{\text{cnv}} + q_{\text{grd}} - q_{\text{sky}} - \frac{1}{2} \cdot q_{\text{vpr}} \quad (15)$$

To find the effects of the double-sided evaporating fabric, simulation results based on Eq. (15) are compared with those based on Eq. (8) in Section 4.1.

4. Simulation results

4.1. Transient simulation for variation of evaporation for a sunny day

Equations (8) and (15) have been solved to find variations of evaporation rate during a sunny day, assuming that the ambient air temperature, humidity, wind speed and sky temperature are constant. The used weather data are listed in Table 1. The daylight duration is 12 h and insolation incident on the fabric has the maximum value of 1.0 kW/m² at noon with a daily total amount of 27.5 MJ/m²-day. The feeding rate m is set to be 2.61 kg/s-m² fabric and 2.41 kg/s-m² fabric for the double-sided and single-sided fabrics, respectively. The initial condition of the fabric temperature T is set to be the same as the value at the end of the day. The simulation model has been run with time intervals of 6 s.

Fig. 2 shows calculated heat fluxes from/to the double-sided evaporating fabric, and fig. 3 does evaporation

Table 1

Weather conditions and constants used for transient simulation.

Ambient air temperature $T_a = 298.15$ K

Sky temperature $T_{\text{sky}} = 288.1$ K

Relative humidity $\phi = 70\%$

Wind speed $u = 5.0$ m/s

Insolation $I = 0$ for $0 < t/3600 < 6$ h and $18 \text{ h} < t/3600 < 24$ h

and $I = 1000 \cdot S_{\text{in}} [(t/3600 - 6)/12]$ for $6 \text{ hr} < t/3600 < 18 \text{ hr}$

Heat capacity of wetted fabric $M \cdot c = 4.2$ kJ/ K-m² fabric

Feeding rate of seawater $m = 0.28 \times 10^{-3}$ kg/s-m² fabric

Inlet concentration $S_{\text{in}} = 3.4$ wt%

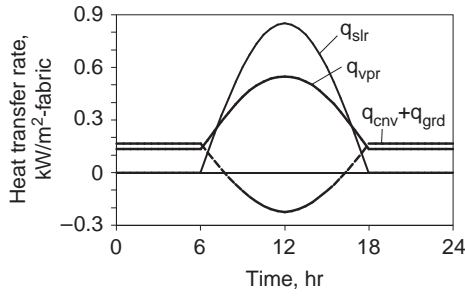


Fig. 2. Variations of heat absorbed or emitted by fabric in a day.

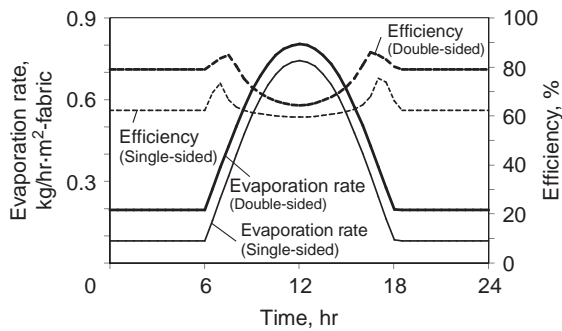


Fig. 3. Variations of evaporation rate and thermal efficiency in a day for single-sided and double-sided fabrics.

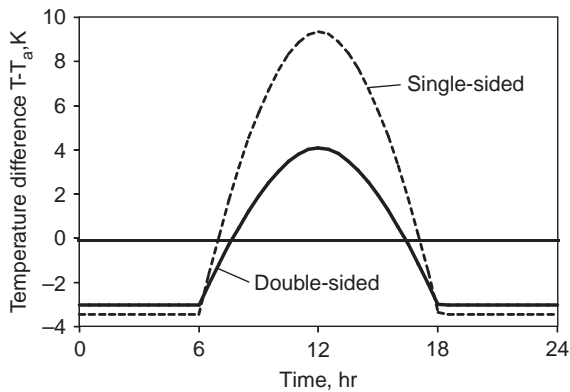


Fig. 4. Variation of fabric temperature in a day for single-sided and double-sided fabrics.

rate and the thermal efficiency of evaporation for both the double-sided and single-sided fabrics. Fig. 4 shows the temperature difference between the fabric and the air ($T - T_a$). The thermal efficiency of evaporation can be defined as

$$\text{thermal efficiency} = \frac{L \cdot m_e}{\text{total heat gained by fabric}} \quad (16)$$

For night time with zero insolation $I = 0$, the fabric cools itself due to evaporation, and gains the heat from the air due to convection q_{cnv} and from the ground due to radiation q_{grd} , which is in proportion to the temperature difference ($T_a - T$) between the surrounding air and the fabric. It emits the same amount of heat due to evaporation and sky radiation. The temperature difference ($T_a - T$) is 3.0 K, and the fabric gains heat equal to $(q_{cnv} + q_{grd}) = 165 \text{ W/m}^2$ from the surroundings. The heat of evaporation q_{vpr} accounts for 78.9% of the total gained heat. The other percentage is the heat loss due to radiation q_{sky} .

For the daytime, the heat from the surroundings ($q_{cnv} + q_{grd}$) decreases with an increasing insolation I , and it is negative, i.e. the fabric emits the heat to the air and the ground as well as the sky for about 9 h from 7:30 a.m. to 4:30 p.m. At noon with $I = 1.0 \text{ kW/m}^2$, the temperature of fabric is higher by 4.1 K than T_a and the heat losses to the surroundings ($q_{cnv} + q_{grd}$) and to the sky q_{sky} are 225 W/m^2 and 74 W/m^2 respectively. The heat of evaporation q_{vpr} accounts for 64.3% of the absorbed insolation of 850 W/m^2 . The enthalpy increase of seawater q_{swt} is only 0.5% of the absorbed insolation because of small amounts of feeding rate m and the temperature difference ($T - T_a$).

For the nighttime, the temperatures of both the fabrics are below the air temperature T_a , and the temperature of single-sided fabric is slightly lower than that of the double-sided one (Fig. 4), since the ratio of the heat loss to sky to the heat gained from the surroundings is larger. The efficiency of evaporation is 78.9% and 62.3% for the double-sided fabric and the single-sided one, respectively (Fig. 3). The evaporation rate is 2.41 times larger for the double-sided fabric than the single-sided one. The double-sided fabric has the double area for evaporation, and the lower surface gains heat from the ground due to radiation as well as the heat from the air due to convection. These cause its higher efficiency and evaporation rate.

For the daytime, the temperature of fabric increases with an increasing insolation, and is higher by 4.1 K and 9.3 K than the air temperature T_a for respectively the double-sided fabric and the single-sided one. The efficiency of evaporation has the maximum at 7:30 a.m. and 4:30 p.m., when the insolation is 325 W/m^2 , the temperature of fabric is close to the air temperature T_a , and thus the total heat loss to the air, ground and sky is a minimum. At larger insolation amounts, the fabric gains heat from the insolation and emits heat to the air, ground and sky. The evaporation rate increases with an increasing insolation, and the maximum evaporation rate is $0.803 \text{ kg/h}\cdot\text{m}^2$ fabric and $0.742 \text{ kg/h}\cdot\text{m}^2$ fabric at noon for the double-sided fabric and the single-sided one,

respectively. The efficiency decreases to a minimum at noon, being 64.3% and 59.4% respectively for the double-sided fabric and the single-sided one. The evaporation rate is larger for the double-sided fabric throughout the day, since its temperature is lower and its total amount of heat loss to the air, ground and sky are smaller.

With the constant feeding rate of 0.940 kg/h-m^2 fabric, the double-sided fabric concentrates seawater from 3.4 wt% to 4.29 wt% for the nighttime and to 23.4 wt% at noon, and the outlet concentration averaged over the day is 5.81 wt%. With the constant feeding rate of 0.868 kg/h-m^2 fabric, the single-sided fabric concentrates seawater to 3.75 wt% for the nighttime and to 23.5 wt% at noon, and the concentration averaged over the day is 5.10 wt%. These results suggest that it is needed to change the feeding rate of seawater with changes in the weather factors for keeping the outlet concentration to be constant at the required value.

The double-sided fabric produces a daily evaporation of 9.37 kg/day-m^2 fabric which is 38% larger than the single-sided one. The simulation shows an evaporation rate of 4.68 kg/day-m^2 fabric assuming zero insolation $I = 0$ for a whole day. The additional effect by insolation is therefore calculated to be $(9.37 - 4.68) = 4.69 \text{ kg/day-m}^2$ fabric. Hereafter, the former and latter productions are called 'basic' evaporation amount, and 'solar aided' or 'additional one', respectively.

4.2. Dependence on weather and operation factors

The evaporation rate m_e is a function of insolation I , humidity ϕ , wind speed u , atmospheric temperature T_a and outlet concentration of the brine S_{out} . Figs. 5(a)–(e) show the variations of the evaporation rate with single weather or operation factors for the double-sided fabric.

The evaporation rate significantly increases from 0.168 kg/h-m^2 fabric to 0.827 kg/h-m^2 fabric with an increase in insolation from 0 to 1.0 W/m^2 . The evaporation rate is zero or negative at $\phi = 0.9$ or larger in Fig. 5(b) because of condensation effect from the humid air into deliquescent brine in fabric. The evaporation rate greatly increases to 0.347 kg/h-m^2 fabric with a decrease in relative humidity ϕ to 50%. It increases with an increasing wind speed u because of a linear relationship between u and the mass transfer coefficient k as expressed by Eq. (13). An increase in u from 2 to 8 m/s causes 2.58 and 2.94 times increases in k and the evaporation rate, respectively. It also increases with an increasing air temperature T_a , and the increase in T_a accompanies with an increase in T_{sky} in Fig. 5(d). The evaporation rate decreases with an increasing outlet concentration S_{out} , and the decrease in evaporation rate is relatively small.

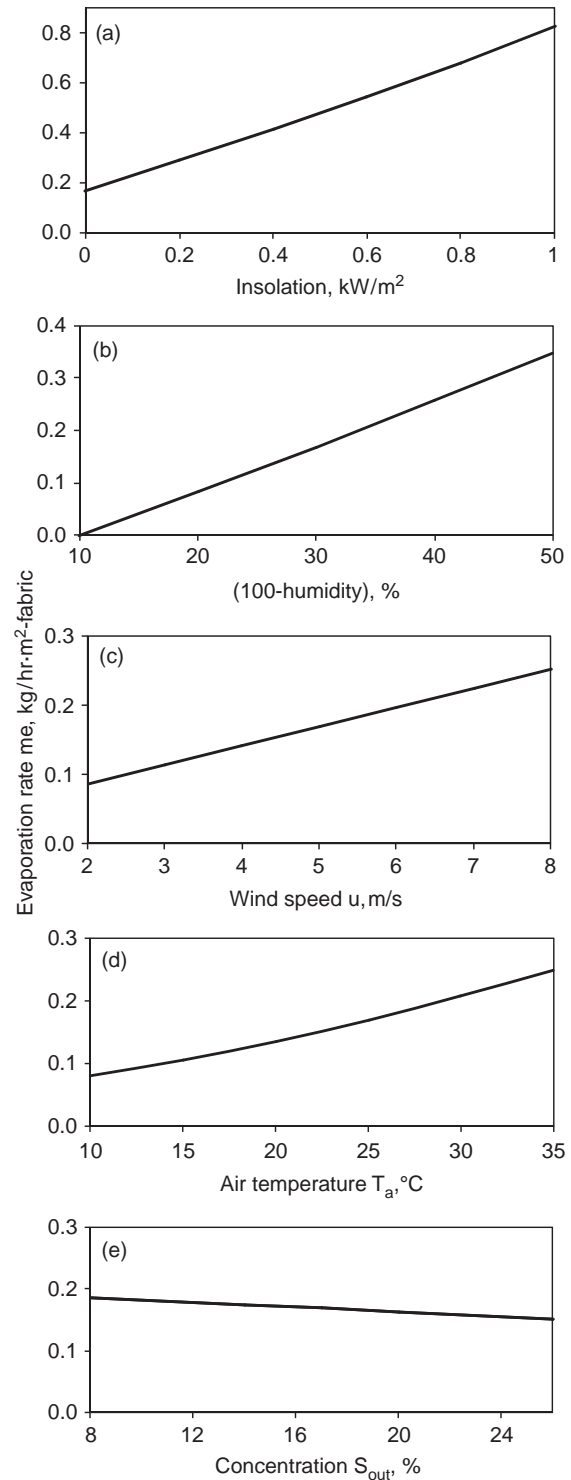


Fig. 5. Variations of evaporation rate with (a) insolation I , (b) relative humidity ϕ , (c) wind speed u , (d) ambient air temperature T_a , and (e) concentration of seawater S . For each variation, the other factors are chosen among $I = 0$, $\phi = 75\%$, $u = 4.0 \text{ m/s}$, $T_a = 293.15 \text{ K}$ and $S_{\text{out}} = 14 \text{ wt}\%$. For the variation with T_a , T_{sky} changes together with T_a as expressed by Eq. (14).

4.3. Variation of evaporation for a year under subtropical and maritime climate conditions

The evaporation rate has been calculated using weather data from the Okinawa Island located at 26° north latitude to the southeast of Chinese Continent. The weather data have been averaged over every month, and then averaged over 30 years of 1971–2000. The averaged data are available from the Japan Meteorological Agency [14], and are shown in Fig. 6. Average atmospheric temperature has the maximum of 301.65 K (28.5°C) in July and the minimum of 293.75 K (16.6°C) in January. The accumulated amount of insolation energy over a day is 20.0 MJ/m²-day in July at the maximum, and is 8.6 MJ/m²-day in January at the minimum. The maximum humidity is 84% in June and the minimum one is 68% in December. The average wind speed is nearly constant and in the range of 5.0–5.5 m/s throughout a year. Okinawa Island has a maritime climate, i.e. the humidity is high and the amount of insolation energy is small because of large amount of cloud cover. Such conditions are not favorable for evaporation.

The average evaporation rate in the nighttime has been calculated using zero insolation $I = 0$ and the averaged weather data shown in Fig. 6. The average evaporation rate in the daytime has been calculated using the same weather data and assuming that incident insolation is constant for the daylight duration and is equal to the daily amount of insolation divided by the daylight duration. The daily evaporation amount is the sum of both the evaporation amounts for the nighttime and daytime.

The basic evaporation amounts are plotted on the graph in Fig. 7, as a function of $(1-\phi)$, showing a hysteresis between the data points for June (at the maximum humidity ϕ) and for December (at the minimum). The hysteresis results from the fact that the ambient air temperature T_a is higher between June and December

when compared to the months of January to June (see Fig. 5(d)).

The additional evaporation from insolation is plotted on the graph in Fig. 8, as a function of the daily amount of insolation. The insolation effect shows the maximum of 3.80 kg/day-m² fabric in July with an insolation energy of 20.0 MJ/m²-day, and the minimum of 1.19 kg/day-m² fabric in January with 8.6 MJ/m²-day. The hysteresis loop is very flat, indicating that the addition by insolation predominately depends on the daily insolation amount and linearly increases with an increasing insolation amount.

Fig. 9 shows the basic, additional and total evaporation amounts for all months, and the values averaged over a year. The total evaporation amount is around a smaller level in the range of 4.51–5.03 kg/day-m² fabric from January to June. It suddenly increases up to the maximum of 6.01 kg/day-m² fabric in July, is around a larger level in the range of 5.54–5.89 kg/day-m² fabric from August to October, and then decreases during November and December. From January to June, the

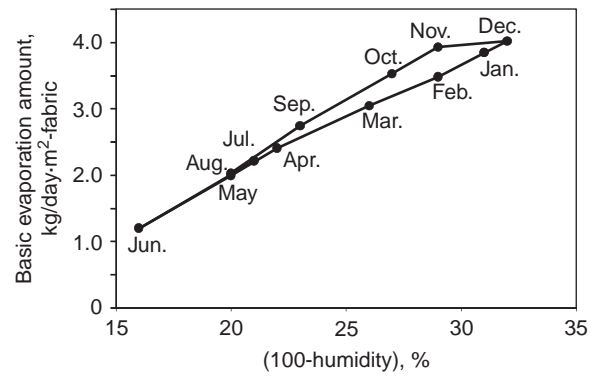


Fig. 7. Basic evaporation amounts in all month plotted as a function of $(1-\phi)$.

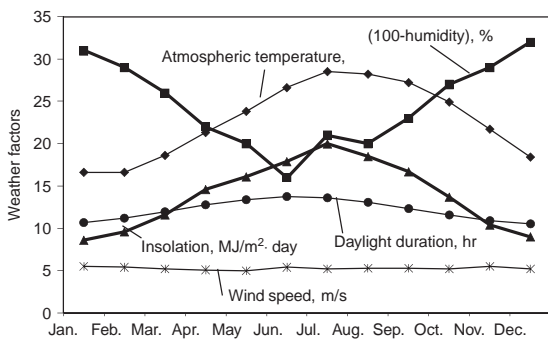


Fig. 6. Weather conditions in all months at Okinawa Island.

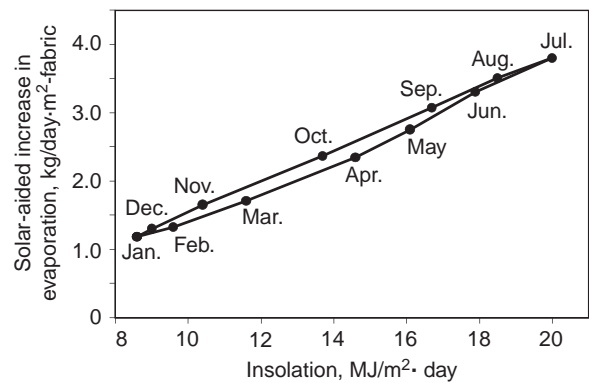


Fig. 8. Additional evaporation amounts due to insolation plotted as a function of insolation amount.

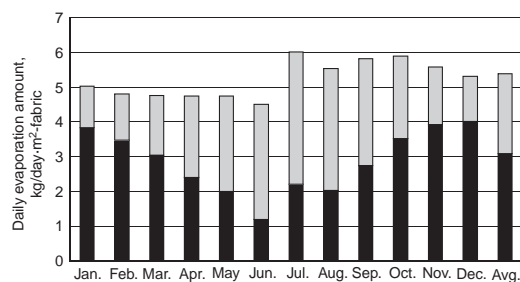


Fig. 9. Column chart of the basic, solar-aided and total evaporation amounts in all months.

increase in the addition by insolation makes up for the decrease in the basic evaporation amount. In most years the rain season ends at the end of June or the beginning of July at Okinawa, causing the sudden increase in the total evaporation in July. From August to December, the increase in the basic evaporation amount makes up for the decrease in the addition by insolation. The addition by insolation is larger than the basic amount for the 5 months from May to September, while the basic one is larger for the 6 months from October to March. When averaged over a year, the daily total, basic and additional evaporation amounts are 5.23, 2.87 and 2.36 kg/day-m² fabric, respectively.

5. Concluding remarks

A double-sided wet fabric evaporator is suggested, which has a potential to concentrate seawater up to a high concentration in a very short fabric length of around 2 m because of a very small flow rate in the fabric of hydrophilic material. Model simulations have been run for evaporation rate under the subtropical and maritime climate conditions of Okinawa Island. The simulation results show that the evaporation from both sides of the fabric effectively cools the fabric, which gains a large amount of heat from the surroundings for the nighttime and emits a small amount of heat loss to the surroundings for the sunny daytime with large insolation. Therefore the suggested evaporator utilizes large percentages of the gained heat and absorbed insolation for evaporation.

The double-sided wet fabric evaporator is predicted to produce an evaporation amount of 5.23 kg/day-m² fabric on average. In summer with large insolation and high humidity, solar-assisted evaporation makes up for the decrease in evaporation due to high humidity. It accounts for 63% of the total evaporation amount of 6.01 kg/day-m² fabric in sunny July. In winter with small

insolation, winds of dry air enhance the evaporation, and this enhancement makes up for the decrease in solar-aided evaporation amount. The solar-aided evaporation accounts for 24% of the total amount of 5.03 kg/day-m² fabric in January. The double-sided wet fabric evaporator produces the minimum evaporation amount of 4.51 kg/day-m² fabric in rainy June, and it is smaller by 14% only than the averaged one, suggesting that this evaporator produces nearly constant evaporation amounts through a year.

These prediction results have encouraged us to construct double-sided wet fabric evaporators, which have been under examinations under real weather conditions at Okinawa Island. In our experiments, a 2 m long fabric has concentrated seawater from 3.4 wt% to 11 wt% during insolation without showing any dry patch on it. The experimental results will be reported in near future.

Acknowledgement

We are indebted to Mr. M. Chinen for his assistance. This research was supported by The Salt Science Research Foundation (Grant # 0611).

Nomenclature

c	specific heat of seawater or seawater-soaked fabric, J/kg-K
h	heat transfer coefficient of fabric, W/m ² -K
I	insolation incident on fabric, W/m ²
k	mass transfer coefficient of fabric, W/m ² -s-Pa
L	latent heat of evaporation, J/kg
M	mass of seawater-soaked fabric per unit area, kg/m ²
m	feeding rate of seawater per unit area, kg/m ² -s
m_e	evaporation rate, kg/s-m ² fabric, see Eq. (7)
p	vapor pressure of seawater, Pa
P_a	partial pressure of water vapor in ambient air, Pa
P_w	saturated vapor pressure of fresh water, Pa
q_{cnv}	convective heat flux to fabric, W/m ² fabric, Eq. (3)
q_{grd}	radiative heat flux from ground to fabric, W/m ² fabric, Eq. (4)
q_{vpr}	loss of latent heat of evaporation, W/m ² fabric, Eq. (6)
q_{sky}	radiative heat flux from fabric to sky, W/m ² fabric, Eq. (5)
q_{slr}	insolation energy absorbed by fabric, W/m ² fabric, Eq. (2)
q_{swt}	enthalpy carried in by feeding seawater, W/m ² fabric, Eq. (1)
S	mean value of S_{in} and S_{out} , kg/kg
S_{in}	concentration of influent seawater, kg/kg
S_{out}	concentration of effluent brine, kg/kg

T	temperature of fabric, K
T_a	ambient air temperature, K
T_{sky}	sky temperature, K
t	time, s
u	wind speed, m/s
α	solar absorptance of fabric
ε	infrared emittance of fabric
σ	Stefan–Boltzmann constant, $W/m^2\cdot K^4$
φ	relative humidity

References

- [1] The Society of Sea Water Science, Japan (SSWSJ) and The Salt Science Research Foundation (SSRF) ed., *Sea Water, its Property and Technology*, Tokai University, Tokyo, 1994, pp. 457–462.
- [2] G. Sugi and M. Nakayama ed., *Chemistry of Sea Salt*, The Society of Sea Water Science, Japan, Tokyo, 1961, pp. 67–73.
- [3] T. Nosoko, T. Kinjo, C. D. Park, Theoretical analysis of multiple-effect diffusion still producing highly concentrated seawater, *Desalination*, 180 (2005) 33–45.
- [4] J. Gilrom, Y. Folkman, R. Savliev, M. Waisman and O. Kedem, WAIV-wind aided intensified evaporation for reduction of desalination brine volume, *Desalination*, 158 (2003) 205–214.
- [5] S. Pancharatnam, Transient behavior of a solar pond and prediction of evaporation rates, *Ind. Eng. Chem. Process Des. Dev.*, 11 (1972) 287–292.
- [6] J.L. Manganaro and J.C. Schwartz, Simulation of an evaporative solar salt pond, *Ind. Eng. Chem. Des. Dev.*, 24 (1985) 1245–1251.
- [7] T.A. Newell, M.K. Smith, R.G. Cowie, J.M. Upper and C.L. Cler, Characteristics of a solar pond brine reconcentration system, *J. Solar Energy Eng.*, 116 (1994) 69–73.
- [8] D.H. Kim, B.M. Jenkins, M.W. Yore and N.J. Kim, Salt recovery from agricultural drainage water using a liquid film solar-assisted concentrator-Simulation and model validation, *Solar Energy*, 81 (2007) 1314–1321.
- [9] K. Srithar and A. Mani, Comparison between simulated and experimental performance of an open solar flat plate collector for treating tannery effluent, *Int. Comm. Heat Mass Transfer*, 30 (2003) 505–514.
- [10] D.H. Kim and B.M. Jenkins, Optimal orientation of liquid-film solar-assisted brine concentrator, *J. Solar Energy Eng.*, 130 (2008) Article no. 024503.
- [11] Japan Society of Mechanical Engineers, *JSME Data Book: Thermal Properties of Fluids*, Japan Society of Mech. Eng., Tokyo, 1985, p. 208.
- [12] R. Witting, *Finlandische Hydrogr.—Biologische Untersuchungen*, no. 2 (1908) 246.
- [13] X. Berger, About the equivalent radiative temperature for clear sky, *Solar Energy*, 32 (1984) 725–733.
- [14] <http://www.data.jma.go.jp/obd/stats/etrn/index.php> (in Japanese)